Controllability of Radial Displacement in Bearingless Switched Reluctance Motor with Bridge Configured Winding

Firdausa Ahmed [a], Karuna Kalita [b]

[a] Centre for Energy, Indian Institute of Technology Guwahati, Guwahati, India, firdausa.ahmed@iitg.ernet.in
[b] Department of Mechanical Engineering, Indian Institute of Technology Guwahati, Guwahati, India

***Abstract*— Due to the salient features of stator and rotor in Switched Reluctance Motor the air-gap of the machine does not remain uniform during its motoring operation. This innate characteristic is responsible in producing considerable amount of radial force in the motor. However on the other hand eccentricity or radial displacement of the rotor is another key cause to this production of radial force. In this paper a single winding structure called bridged configured winding in a 12/8 BSRM is delineated which can be used to deploy the radial displacement by injecting controlled current within the same winding. Initially a mathematical model of the motor is developed and verified using finite element modeling. The developed model is analyzed by integrating a voltage source asymmetric converter for motoring operation and separate asymmetric converters for injecting currents into the winding to control the radial displacement of the motor. Investigations of radial forces at various rotational positions and controllability of radial displacement are carried out using a simple PID controller system.**

I. INTRODUCTION

Switched Reluctance Motors have found its extensive usage in the field of high speed application due to its simpler structure and variable speed range. However due to continuous friction the life of bearings are shortened which further limits the wide application of SRMs. As a solution to this bearingless technology has been combined with SRMs which helps them to operate as a normal motor but with both the shaft and rotor levitated. The main feature of SRMs which helps them to be convertible as BSRM is their inherent capability of producing substantial amount of radial force while in its operation. Researchers have published numerous solution of producing radial force [1] where two sets of winding occupy the same stator pole, one winding for the torque production and the suspension winding for radial force and the current in each winding is adjusted to produce both torque and force. [2-4] have proposed various methods of radial force production but they require many suspension windings which results in usage of space in stator slots which could have been otherwise used for torque production. The additional use of suspension winding again increases the need of power converters for each phase.

Dual set of winding was introduced for bearingless switched reluctance motor where two sets of winding are embedded on the same stator. One is the motor's main winding which is responsible for rotation of the machine and the other is a secondary stator winding responsible for providing the suspension force to the rotor [1]. Various researchers have published works about BSRMs [1-5] which require many suspension windings viz. for a three phase motor a total of six set of suspension winding is required. As a result the number of power converter circuitry increases thus complicating the control scheme. Again few researchers have worked on the integration of magnetic bearing and mechanical bearing with SRM [6]. However these methods were not reliable in case of high speed applications because of the problems associated with mechanical bearings. Hybrid structure of BSRM was also proposed by researchers which had separate poles for torque and radial force [6]. In 2006, a novel BSRM using a single winding structure was developed where three phases were loaded with different current at the same time in order to produce force and torque. They analytically computed currents in the winding and derived its relation with radial force and torque [7]. In 2010, the same researchers did an analysis under eccentric condition of the motor. They made a calculation of air-gap such that the eccentric force does not exceed the maximum levitation forces in the windings [8]. In 2011, this single winding structure was practically tested for an 8/6 SRM to validate the theoretical relations obtained [9,10]. In 2007 single-phase and two-phase sinusoidal excitation was tested in a 12/8 single winding based BSRM to regulate the torque and radial force but the control scheme was complicated for levitation and rotation [11]. Independent control of both torque and radial force strategy was introduced by using hybrid excitations in the main windings and levitation windings in each phase. But one disadvantage of this technique was that a negative torque was produced in each phase as the descending inductance region was used for levitation [12]. However, in 2005 a single set of winding called bridge configured winding (BCW) was introduced for poly-phase self-bearing machines which could generate both the torque and the radial force using the same winding. The nature of this winding is such that the currents responsible for producing torque is divided into two parallel paths and an isolated power supply, called bridge current power supply is introduced at the midpoint of the path to produce a net radial force. With the bridge current supply terminated, the motor could operate as a normal torque producing machine [13, 14].

In 2016 the concept of bridge configured winding (BCW) was introduced in SRM for both torque and radial force production. This design was a promising development which could produce both rotating torque and radial force using a single set of winding [15]. This design was further analyzed for a 12/8 SRM considering magnetic saturation of the motor and obtained a mathematical model of the proposed design [16]. In 2017 a design methodology was proposed for proper selection of the geometrical parameters that contribute towards achieving the minimum levitation force at every orientation of rotor and reduce the complexities associated with bearingless operation. They worked on the geometrical structure of BSRM to predict the minimum stator-rotor overlap angle in order to obtain the minimum required force for levitation at every rotational position [17].

This paper proposes a single winding structure called bridge configured winding for BSRM which is capable of producing both torque and controllable radial force with the help of minimal current injection in between the windings and thus control the radial displacement of the rotor. Initially an analytical model has been developed by solving the flux paths using Maxwell Stress Tensor method and the relations of torque, radial force and the currents are obtained by considering change in length of air-gap due to displacement of rotor [12]. In order to verify the analytical relations a finite element model has been designed and developed in ANSOFT Maxwell 2D. In order to drive the motor a voltage source asymmetric bridge converter circuit is designed in the external circuit editor platform of Maxwell 2D and coupled with the FE model for transient analysis. The analysis has been done considering a small eccentricity in the air-gap of the motor. In order to produce an opposite radial force in the motor an external converter circuit is developed and current called bridge current from it is allowed to flow through the windings. The radial force produced due to the bridge current helps in cancelling the eccentric radial force produced and nullify the displacement produced due to it. This controllability is shown with the help of a PID controller built in Matlab/SIMULINK.

II. STATOR WINDING DESIGN METHODOLOGY

A conventional SRM having 12 slots in stator and 8 slots in rotor is selected as the prototype for bridge configured stator winding. Fig.1 shows the schematic of a 12/8 teeth SRM with the coil arrangements for bridge configured winding and Fig.2 shows the connection of the phase windings with the main power supply and the bridge current power supply.

A. Bridge Configured Winding for BSRM

Bridge configured winding (BCW) is a specialized single set of stator winding containing double layer of coils in each stator teeth and connected in the form of Wheatstone bridge configuration. The principle feature of this winding is that it has two sets of terminal connection at its end winding, one terminal for connecting the torque producing circuit and another for radial force producing circuit. The main current which produces the machine torque is divided into two parallel paths and a small bi-directional supply at the midpoint of these two paths provides the current responsible for production of the radial forces. This small isolated supply is referred to as the bridge power supply and the currents as the bridge currents.

A conventional SRM having 12 slots in stator and 8 slots in rotor is selected as the prototype for the bearingless operation of the motor by introducing bridge configured stator winding. Fig.1 shows the schematic of a 12/8 teeth SRM with the coil arrangements for bridge configured winding and Fig.2 shows the connection of the phase windings with the main power supply and the bridge current power supply. The currents i_{b1} and i_{b2} as shown in Fig.2 represents the bridge currents which are responsible for producing radial force in any desirable direction. This possibility of the bridge currents to produce equal and opposite radial force has been explored in this paper when there is any eccentricity in the air-gap of the motor.

The 12/8 SRM chosen for BCW requires a 3-phase converter circuit for its operation where each phase leg consists of coils of one phase winding. As seen in Fig.2 phase-A consists of coils where coil set (1a-7a′)-(7a-1a′) and (10a-4a')-(4a-10a') form the two parallel paths of the winding.1a and 1a' constitute a coil set with same number of turns and occupy a stator tooth while coil set 7a and 7a' occupy diametrically opposite stator tooth. Coil set 4a-4a' and 10a-10a' occupy the stator slot which are 90 degree apart with respect to coil set 1a-1a' and 7a-7a' as shown in Fig.1. Similarly the Phase-B constitute of the coil sets (2b-8b′)-(8b-2b′) and diametrically opposite set (11b-5b′)-(5b-11b′) and Phase-C constitute of coil sets (3c-9c′)-(9c-3c′) and diametrically opposite coil set (12c-6c′)-(6c-12c′). The points (a_1-b_1) and (c_1-d_1), (a_2-b_2) and (c_2-d_2), (a_3-b_3) and (c_3-d_3) represents the terminal points of phase-A, B and C of the winding where the bridge currents i_{b1} and i_{b2} can be injected for the force production as shown in Fig.2. For this configuration, the power converter circuits required for the bridge currents per phase is two.

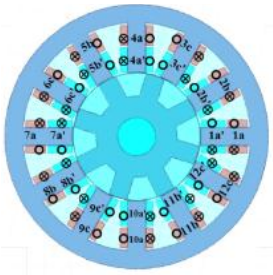

Figure 1. Schematic of 12/8 BSRM with BCW

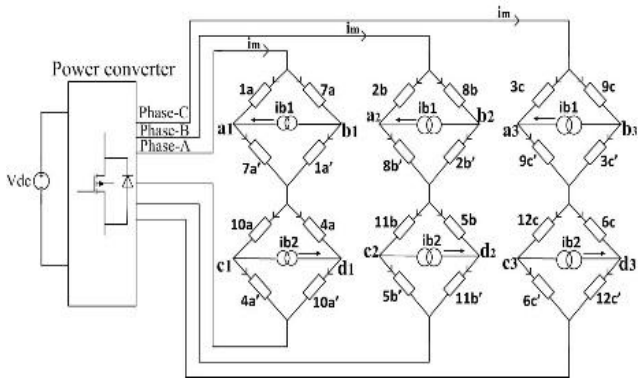

Figure 2. Connection of coil terminals for main current i_m and bridge currents i_{b1} and i_{b2}

B. Mathematical Relation of Torque and Radial Force Considering Rotor Radial Displacement

Figure 3 shows a 12/8 bridge configured winding in BSRM with only phase-A winding configuration where A_1, A_2, A_3 and A_4 represents the stator poles of phase-A winding. Figure 4 shows the arrangement of coils and the connection of the main current supply (i_m) and bridge current supply (i_{b1} and i_{b2}). The arc of the rotor tooth is taken as 17^0 and the stator tooth as 16^0. The aligned position of the stator and rotor is defined as $\theta=0^0$. When the main current, i_m conducts in the phase-A winding in the direction as shown in Fig.4, the magnetic field formed is of four poles keeping the flux densities in the four air-gaps equal. In this case the motor operates as a normal rotating machine. The conduction period (θ_c) for each phase is kept as 15^0.

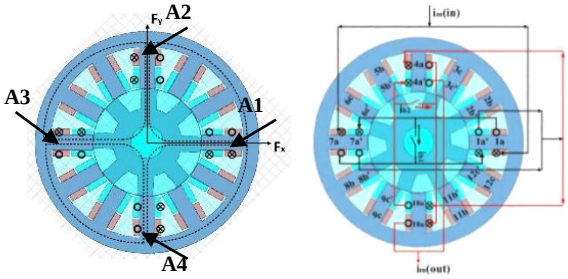

(a) (b)

Figure 3. (a) Four pole magnetic field in phase-A (b) Physical representation of bridge winding connection for Phase-A

The current gets added in the coils where the direction of flow of main current i_m and i_{b1} is same and current gets deducted in the coils where the direction of i_{b1} is opposite to i_m. Hence an unbalance is created which creates a magnetic force in the direction of positive x - axis. Similarly, a radial force can be created in the direction of y-axis when current i_{b2} is supplied as shown in Fig.4. Thus by operating the bridge currents, required radial force can be created in any desired direction. The radial force produced by phase B and C can be obtained similarly. Figure 4 shows the flow of main current and bridge current through the coils when the terminals are connected in a bridge manner. The main current gets divided and enter the coils i.e. each coil carries half of the main current i_m and half of the bridge currents i_{b1} and i_{b2}. Whenever there is any imbalance in the magnetic field of the system due to rotor eccentricity, then with the help of these bridge currents, equal radial force can be produced in the desired direction and help in providing a balanced magnetic field. Hence, in order to determine the actual amount of current required to produce the radial force a relationship between force and current with respect to rotor displacement is mandatory.

In Maxwell stress tensor, the expression of resultant force is obtained from the flux density in the air-gap generated by the currents in the winding.

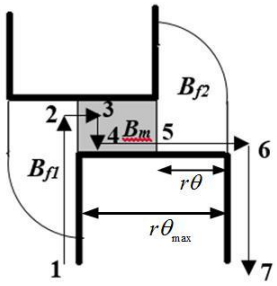

Figure 4. Integration of main flux path and fringing flux paths

According to Maxwell stress tensor method, the force per unit area along a certain dimensional mechanical angle on the rotor surface can be expressed as,

$$dF(\theta)=\frac{B^2(\theta)dS}{2\mu_0} \tag{1}$$

where, μ_0 is the permeability of air, S is the area of air-gap, θ is the rotor rotational position in mechanical degree and B is the magnetic flux density[12].

The normal and tangential force acting on the rotor can be given as,

$$F_n=\frac{1}{2\mu_0}\iint_S (B_n^{\,2}-B_t^{\,2})dS \tag{2}$$

$$F_t=\frac{1}{\mu_0}\iint_S (B_nB_t)dS \tag{3}$$

The length of the integral path can be expressed as

$$\begin{aligned} l_{34}&=l_0\\ l_{23}+l_{45}&=r\theta_{\max}-r\theta\\ l_{56}&=r\theta \end{aligned} \tag{4}$$

where, $\theta_{\max}$ is the rotor arc angle, r is the radius of the rotor and l_o is the length of the air-gap.

The radial force component can be given as,

$$F_r = \frac{h}{2\mu_0}\left(\int_2^3 B_m{}^2 dl + \int_4^5 B_m{}^2 dl + \int_5^6 B_{f2}{}^2 dl\right) \quad (5)$$

And the tangential force component equals

$$F_t = \frac{h}{2\mu_0}\left(\int_1^2 B_{f1}{}^2 dl - \int_3^4 B_m{}^2 dl\right) \quad (6)$$

where *h* is the stack length of the rotor.

The torque acting on the rotor pole in Fig.6 can be written as

$$T = F_t r = \frac{hr}{2\mu_0}\left(B_{f1}{}^2 l_{12} - B_m{}^2 l_{34}\right) \quad (7)$$

The current flowing through each stator pole of phase-A is given as,

TABLE I. CURRENT DISTRIBUTION IN PHASE-A

Stator poles(coil numbers)	Current distribution
A1(coils 1a and 1a′)	$I_1 = i_m + i_{b1}$
A2(coils 4a and 4a′)	$I_2 = i_m + i_{b2}$
A3(coils 7a and 7a′)	$I_3 = i_m - i_{b1}$
A4(coils 10a and 10a′)	$I_4 = i_m - i_{b2}$

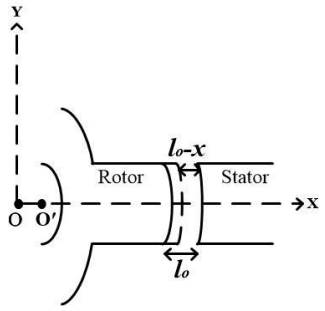

Figure 5. Change in air-gap length due to rotor displacement in positive x-direction

With rotor displacement in the *x*-direction a displacement of *x mm* is considered and the air-gap length is then taken as (l_o-*x)* in the positive *x*-direction and (l_o+*x)* in the opposite x-direction. Figure 5 shows the centre of the rotor and the stator as *O*, when there is no eccentric displacement of the rotor. But with shift in position of the rotor along the *x*-axis, the rotor's central position shifts to *O'* as shown.

The main flux density at air-gap A_1 and A_3 can be obtained from the straight flux lines as

$$B_{ma1} = \frac{\mu_0 N I_1}{l_0 \pm x} \quad (8)$$

and

$$B_{ma3} = \frac{\mu_0 N I_3}{l_0 \pm x} \quad (9)$$

where, *N* is the number of turns per pole and I_1 and I_3 are the net currents at pole A_1 and A_3.

The fringing flux densities can be obtained from the circular and straight flux lines as

$$B_{fa1} = \frac{\mu_0 N I_1}{l_0 + \frac{\pi}{4} r\theta \pm x} \quad (10)$$

$$B_{fa3} = \frac{\mu_0 N I_3}{l_0 + \frac{\pi}{4} r\theta \pm x} \quad (11)$$

The radial force acting on pole A_1 and A_3 is given as,

$$F_{a1} = \frac{B_{ma1}{}^2 A}{2\mu_0} + \frac{B_{fa1}{}^2 A}{2\mu_0} = \frac{\mu_0 hrN^2}{2}\left[\frac{\theta_{\max} - \theta}{(l_0 - x)^2} + \frac{16\theta}{(4l_0 - 4x + \pi r\theta)^2}\right] I_1^2 = K_{f1} i_m{}^2 \quad (12)$$

$$F_{a3} = \frac{B_{ma3}{}^2 A}{2\mu_0} + \frac{B_{fa3}{}^2 A}{2\mu_0} = \frac{\mu_0 hrN^2}{2}\left[\frac{\theta_{\max} - \theta}{(l_0 + x)^2} + \frac{16\theta}{(4l_0 + 4x + \pi r\theta)^2}\right] I_3^2 = K_{f3} i_m{}^2 \quad (13)$$

where, B_m is the field density due to main flux path, B_f is the fringing flux field density, θ_{max} is the rotor tooth arc angle, *h* is the stack length, *N* is the number of turns in each stator tooth, *x* is the displacement in air-gap, l_0 is the air-gap length, *r* is the radius of the rotor and i_m is the main current.

Thus the net radial force produced by phase-A on *x*-axis direction can be given as,

$$F_x = F_{a1} - F_{a3} = (K_{f1} - K_{f3}) i_m{}^2 \quad (14)$$

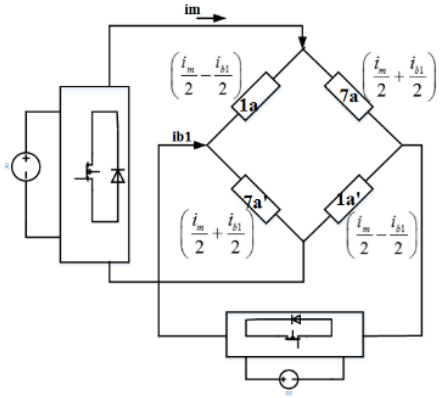

Figure 6. Injection of bridge current i_{b1} in poles *A1* and *A3*

By injecting a bridge current i_{b1} in between poles A_1 and A_3, the net radial force in opposite x-direction can be given as,

$$\begin{aligned} F_x' &= F_{a3} - F_{a1} \\ &= \frac{\mu_0 N^2 hr}{2}\left[\frac{\theta_{\max}-\theta}{(l_0+x)^2}+\frac{16\theta}{(4(l_0+x)+\pi r\theta)^2}\right] I_3^{\,2} \\ &\quad -\frac{\mu_0 N^2 hr}{2}\left[\frac{\theta_{\max}-\theta}{(l_0-x)^2}+\frac{16\theta}{(4(l_0-x)+\pi r\theta)^2}\right] I_1^{\,2} \end{aligned} \tag{15}$$

where, $I_1 = i_m - i_{b1}$ and $I_3 = i_m + i_{b1}$

III. ASYMMETRIC BRIDGE VOLTAGE SOURCE CONVERTER CIRCUIT FOR THE BSRM DRIVE

The driving method of the Switched Reluctance Motor requires a power converter circuit in the input supply which provides switched power supply in each phase. The driver circuit used in this paper for producing torque in the bridge configured SRM is the conventional three phase voltage source asymmetric bridge converter. A 12/8 pole normal SRM is proposed in this paper to integrate bridge configured winding and operate it as a bearingless motor. Each phase is connected to four stator tooth placed diametrically opposite to each other and each phase is excited separately and sequentially as shown in Fig.2.

The voltage source converter used in this paper is the conventional asymmetric bridge converter used for producing only torque in the motor. It consists of three phase legs where each phase is connected to the phase windings. Each leg consists of two switches (MOSFETs or IGBTs) and diodes for freewheeling the energy stored in the inductor. A 100V dc source is used as the voltage supply and the switches are operated by applying a PWM controlled square wave signal. In order to avoid negative production of torque the switching of the phases has to be fast. Since it is a 12/8 motor hence, for one complete rotation of the rotor it has to traverse $\frac{2\pi}{8}$ degree i.e. 45^0.

For a 3-phase driver circuit the conduction period (θ_c) has to be fixed as 15^0. In switched reluctance motor maximum torque is obtained at the position of increasing inductance and is minimum at the position of complete alignment of the stator and the rotor tooth. As such, an initial starting position of Phase-A is chosen when the rotor is completely unaligned with the stator and set for initial excitement. The model of the motor is designed in ANSOFT Maxwell 2D and the converter circuit is modeled in Maxwell circuit editor and integrated with the machine model. The model is simulated in transient mode, where the winding current shifts from phase-A to phase-B after a period of 15^0 rotation and similarly to phase-C. In this study the motor is operated at a rated speed of 1500rpm and based on the rotational speed the time required to complete a 15^0 mechanical rotation is calculated. The duty ratio of the PWM control signal is assigned maintaining the time required to complete one 15^0 rotational period for each phase.

Thus, the time required to traverse an angle of 15^0 is calculated as,

$$\begin{aligned} t_r &= \frac{15}{\frac{1500}{60}\times 360} \\ &= 1.66ms \end{aligned} \tag{16}$$

And the time required for one full conduction i.e. 45^0 is given as,

$$\begin{aligned} T &= \frac{45}{\frac{1500}{60}\times 360} \\ &= 5\text{ms} \end{aligned} \tag{17}$$

Here, t_r is the time required to keep the signal ON i.e. the pulse width of the signal and T is the total time of ON and OFF period.

The pulse width is kept as 1.66ms if expressed in terms of time in order to traverse an angle of 15^0 in each phase and the total time period of the signal is 5ms. Thus the duty ratio of the PWM switching signal is calculated as,

$$Duty\ ratio = \frac{t_r}{T} = 33.2\% \tag{18}$$

TABLE II. SEQUENCE OF PHASE CONDUCTION

Phase windings	Conduction period (θc)	Switches
Phase-A	0-15^0	S_1,S_2
Phase-B	15^0-30^0	S_3,S_4
Phase-C	30^0-45^0	S_5,S_6

TABLE III. DIMENSIONS OF MOTOR

Parameters	Values
Stator outer diameter, D_o	136 mm
Back of core thickness, C_s	9.28 mm
Height of stator tooth, h_s	25.52 mm
Stack length, h	53mm
Stator tooth arc angle, β_s	16 degree
Air –gap length, l_0	0.5mm
Number of turns per coil, N	20
Rotor outer diameter, D_r	65.4mm
Height of rotor tooth, h_r	13.44m
Rotor tooth arc angle, β_r	17 degree
Rotor yoke thickness, C_r	11.15mm
Shaft diameter, D_{sh}	16.7mm
Rotor Displacement, x	0.05mm
Mass of the rotor system	1.2kg

A. Compensation of Radial Force using bridge current

With the integration of the converter circuit with the model the motor is simulated for a transient period. The main current through the winding starts flowing, producing a torque in the motor but as there is a change in air-gap length due to the rotor displacement a radial force is also generated along the direction of x-axis. Figure 7 shows the plot of the main current flowing through the motor winding in Phase-A, Phase-B and Phase-C for a 30^0 rotation.

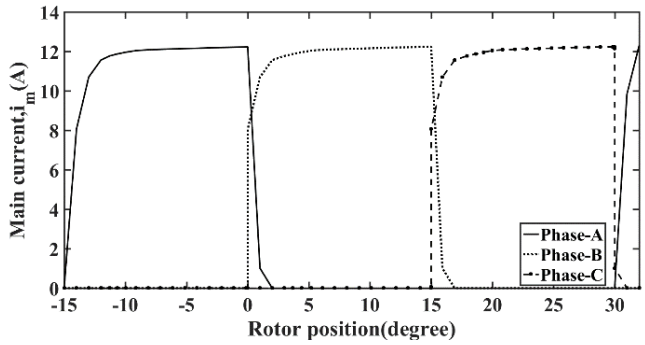

Figure 7. Main current i_m for Phase-A, Phase-B and Phase-C conduction

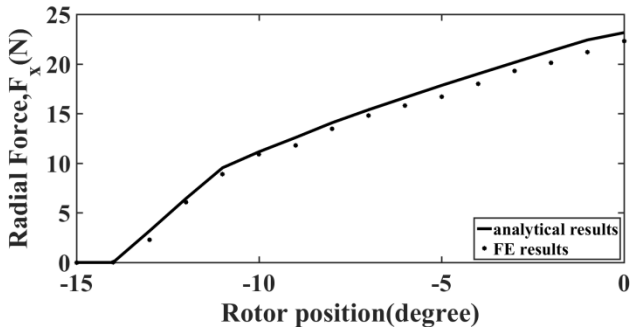

Figure 8. Comparison of radial force in *x*-direction from analytical and FE results for Phase-A

Figure 8 shows the plot of the radial force produced due to eccentricity in air-gap in the positive *x*-direction. The analytical relation of radial force as obtained from Eqn.(14) is compared with a FE analysis of the model and the results obtained are of significant match. In order to produce an equal and opposite radial force, the terminals at the bridge point of the winding are used for injection of bridge currents i_{b1} as shown in Fig. 9.

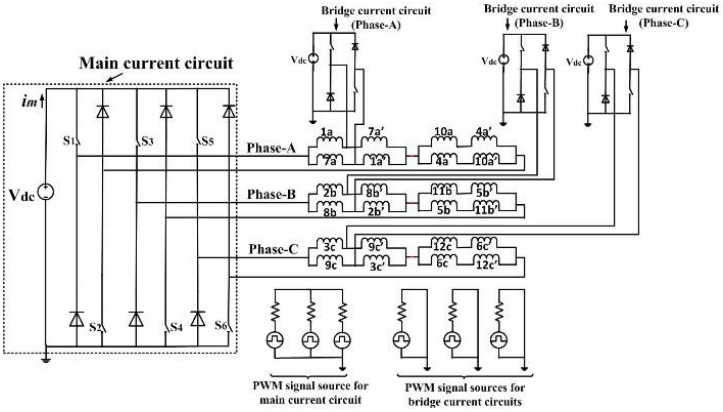

Figure 9. Asymmetric bridge converter for main current i_m and bridge current i_{b1}

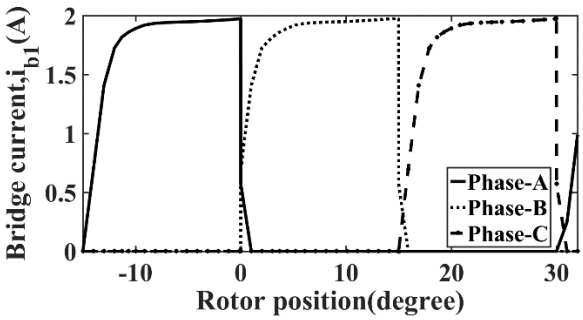

Figure 10. (a) Bridge current i_{b1} in Phase-A, Phase-B and Phase-C

Figure 10 shows the profile of bridge current i_{b1} flowing through the mid- point terminals of the motor winding in Phase-A, Phase-B and Phase-C. The circuit for the bridge current is connected as shown in Fig.9 which creates a net radial force in the opposite *x*-direction. The results plotted for the radial force in Fig. 11 are of significant match with results as obtained in Fig.8.

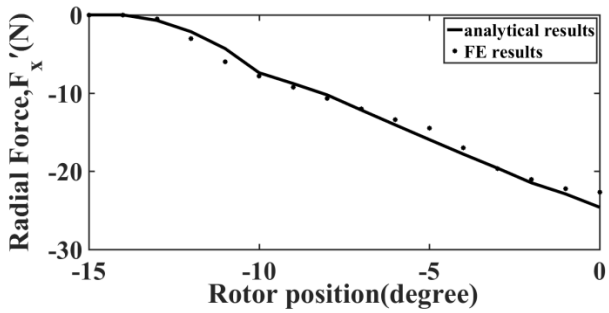

Figure 11. Comparison of radial force in opposite *x*-direction (F_x') from analytical and FE results of Phase-A

B. Controllability of Rotor displacement using PID controller

The main objective of this study is to nullify the effect of any external disturbance and control the radial displacement of the rotor and shaft. As such a closed loop control of the system is necessary. The capability of the bridge current is explored which can produce an equal and opposite radial force by decreasing current in the coil towards which the

shaft gets displaced and by increasing the current in the opposite coil.

Assuming a main current i_m and bridge current $i_{b1,}$ the required radial force can be represented as,

$$F_x^{'} = \frac{\mu_0 N^2 A_g}{2(l_g + x)^2}(i_m + i_{b1})^2 - \frac{\mu_0 N^2 A_g}{2(l_g - x)^2}(i_m - i_{b1})^2 \quad (19)$$

where, A_g is the area of the air-gap and x is a small displacement in air-gap.

From the above equation it is observed that it comprises of two independent variables, the displacement x and the bridge current i_{b1}, assuming the main current and the rotational position known.

Linearising Eqn (19) for a small change in force Δf, for a small displacement Δx and a small control bridge current Δi_{b1} using taylor series,

$$\Delta f = \frac{\partial F'}{\partial x}\Delta x + \frac{\partial F'}{\partial i}\Delta i_{b1} \quad (20)$$

After partial differentiation of F′ with respect to x and i_{b1}, it can be written as,

$$\begin{aligned} F' = & \left[\frac{\mu_0 hrN^2}{2}\left(\frac{-2(\theta_m - \theta)}{(l_0 + x)^3} - \frac{128\theta)}{(4l_0 + 4x + \pi r\theta)^3}\right)(i_m + i_{b1})^2\right]\Delta x - \\ & \left[\frac{\mu_0 hrN^2}{2}\left(\frac{2(\theta_m - \theta)}{(l_0 - x)^3} + \frac{128\theta)}{(4l_0 - 4x + \pi r\theta)^3}\right)(i_m - i_{b1})^2\right]\Delta x - \\ & \left[\mu_0 hrN^2\left(\frac{(\theta_m - \theta)}{(l_0 + x)^2} + \frac{16\theta}{(4l_0 + 4x + \pi r\theta)^2}\right)(i_m + i_{b1})\right]\Delta i_{b1} - \\ & \left[\mu_0 hrN^2\left(\frac{(\theta_m - \theta)}{(l - x)^2} + \frac{16\theta}{(4l_0 - 4x + \pi r\theta)^2}\right)(i_m - i_{b1})\right]\Delta i_{b1} \end{aligned} \quad (21)$$

Hence Eqn. 20 can be written in the form as,

$$\Delta f = -k_x \Delta x + k_i \Delta i_{b1} \quad (22)$$

where, k_x is the open loop stiffness and k_i is the gain of the current in the winding.

Considering the dynamics of the rotor system, the equation of the system can be written as,

$$\Delta f = m\frac{d^2\Delta x}{dt^2} \quad (23)$$

Comparing Eqn.22 and Eqn. 23 we get,

$$m\frac{d^2\Delta x}{dt^2} + k_x \Delta x = k_i \Delta i_{b1} \quad (24)$$

Taking Laplace's transformation on both sides,

$$ms^2\Delta x(s) + k_x \Delta x(s) = k_i \Delta i_{b1}(s) \quad (25)$$

Thus the control equation or the transfer function of the system can be given written as,

$$\frac{\Delta x(s)}{\Delta i_{b1}(s)} = \frac{k_i}{k_x + ms^2} \quad (26)$$

Here in this paper as a rotating body is considered which has the ability to create a levitation force hence the open loop stiffness gain and the current gain are determined at every position of the rotor where radial force is produced. As each phase conducts from the position when the rotor is unaligned to an aligned position with the stator, force is produced accordingly for every phase conduction.

The PID controllers are the most widely used for closed loop control of magnetic levitation and bearingless systems. In this paper a PID based feedback control is used because of its simplicity and easy realization. The simulation model is designed and modeled in SIMULINK/MATLAB environment.

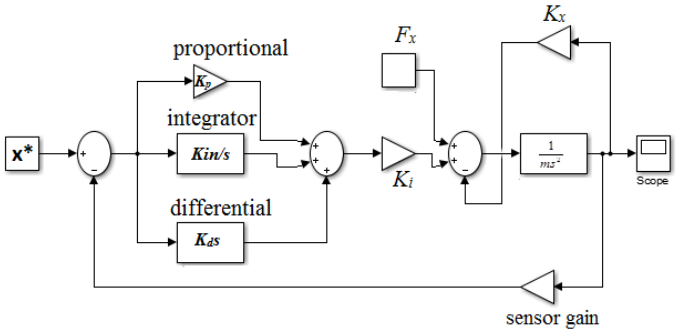

Figure 12. Simulink block of a PID controller with the system

Figure 12 shows the block diagram of a PID controller where x* is taken as the reference of the displacement. The position error e_x is added to the PID controller so that the force command F_x^* is generated[1]. The force tries to move the rotor to its opposite direction to the x-axis thus gradually reducing the displacement x. The output of the controller decreases until the position is on the reference and gives zero position error. The values of the controller gains viz. K_p, K_i and K_d are varied and simulated in order to obtain the best response of the system. The response of the system is checked for varying values of rotor position (θ). Figure 13 shows the response of displacement when the rotor position is at complete aligned position with the stator i.e. at 0^0 position. The controller gains are taken as, K_p=10,K_d=0.01 and varying the value of K_i at 100 and then 1000. It can be observed that when K_i=100 the response of displacement is slow. Therefore the best response is obtained at K_i=1000.

Figure 13, fig 14 and fig 15 shows the displacement response at (0^0) degree (completely aligned), (-5^0) degree (mid-aligned) and (-10^0) degree (semi-aligned) rotor position with the stator.

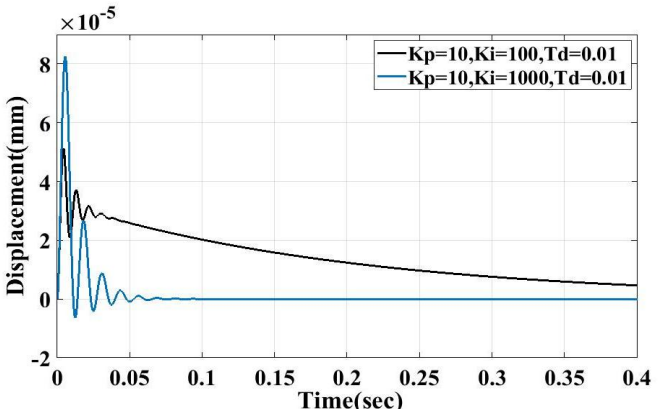

Figure 13. Response of radial displacement at aligned position ($\theta = 0^0$)

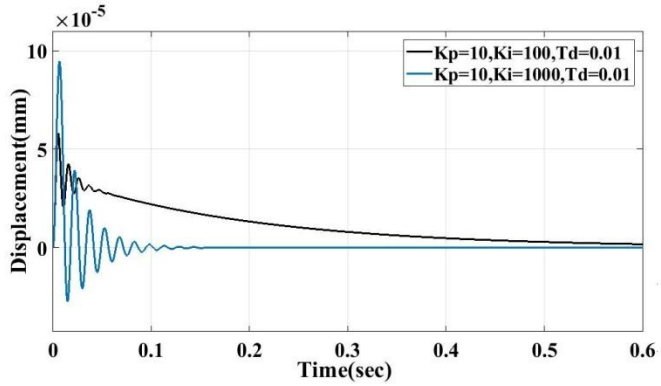

Figure 14. Response of radial displacement at aligned position ($\theta = -5^0$)

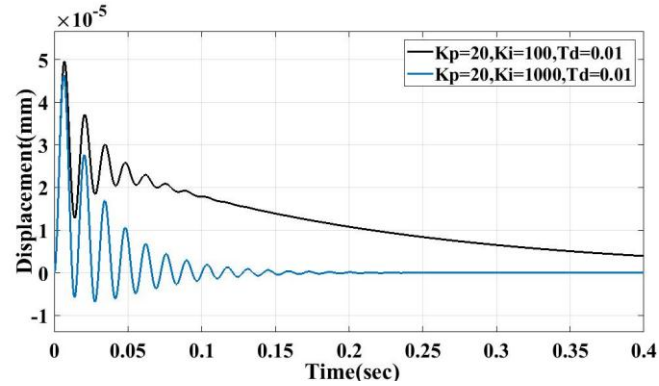

Figure 15. Response of radial displacement at aligned position ($\theta = -10^0$)

From the results obtained from the displacement response curves, it can be observed that higher values of controller gains result in a fast response for a small displacement. Using this feedback loop, the rotor for any eccentric displacement can be controlled using the method of bridge current injection in the windings, reducing the additional use of magnetic bearing or separate suspension winding for the radial force production.

IV. CONCLUSIONS

In this paper, a winding configuration has been proposed and designed which is capable of producing controllable radial force and torque within the same winding. This design methodology has been exploited under condition of static rotor eccentricity. An expression of radial force is developed using Maxwell stress tensor method from which the bridge currents can be calculated required to produce the radial force in opposite direction under eccentric condition. The analytical model expresses the mathematical relationship between the radial force, the main current and the bridge current in the windings for every rotational angle with eccentric displacement. A Finite Element (FE) model has been designed which has been integrated with separate converter circuits as supply for main current and bridge current in the windings and analyzed under transient conditions using Ansoft Maxwell 2D. The results obtained from the analytical relations have been verified with the FE results of the model. The bridge current has been taken into account which can produce an equal and opposite force and thus compensate the radial force produced due to rotor and shaft displacement and bring the rotor back to its position. A simple PID controller has been designed for the control of the eccentric rotor at various rotational positions. The results obtained gives a significant approach to the control of the rotor displacement under eccentric condition using the bridge current injection within the same winding along with a closed loop PID controller.

In this paper, separate hardware converter circuits have been discussed for the production of levitation currents. The design can be made compact by further extending it to a firmware or microcontroller based driver circuit thus giving a wider application to the bearingless motor system.

REFERENCES

[1] Chiba, A., Fukao, T., Ichikawa, O., Oshima, M., Takemoto, M., and Dorrell, D., Magnetic Bearings and Bearingless Drives, Oxford, UK: Elsevier Science, Chaps. 1, 3, and 15, 2005.

[2] Takemoto, M., Shimada, K., Chiba, A., and Fukao, T. "A design and characteristics of switched reluctance type bearingless motors," *Proc. Int. Sym. Magn. Suspension Technol*., Vol. NASA/CP-1998-207654, pp. 49–63, 1998.

[3] Takemoto, M., Chiba, A., and Fukao, T., "A method of determining the advanced angle of square-wave currents in a bearingless switched reluctance motor," *IEEE Trans. Ind. Appl*., Vol. 37, No. 6, pp. 1702–1709, November/December 2001.

[4] Takemoto, M., Chiba, A., Akagi, H., and Fukao, T., "Radial force and torque of a bearingless switched reluctance motor operating in a region of magnetic saturation," *IEEE Trans.Ind.Appl*.,Vol.40, No. 1, pp. 103–112, January/February 2004.

[5] Takemoto, M., Suzuki, H., Chiba, A., Fukao, T., and Rahman, M. A., "Improved analysis of a bearingless switched reluctance motor," *IEEE Trans. Ind. Appl*., Vol. 37, No. 1, pp. 26–34, January/February 2001.

[6] Lee, D. H., Wang, H. J., and Ahn, J. W., "Modeling and control of novel bearingless switched reluctance motor," *IEEE Energy Conversion Congress Expo*, Vol.1-6, pp.685-690, 2009.

[7] L. Chen and W. Hofman, "Analytically computing winding currents to generate torque and levitation force of a new bearingless switched

reluctance motor," in *Proc. 12th Int. Power Electronics and Motion Control Conference*, Portoroz Slovenis, 2006, pp.1058-1063.

[8] Chen, L., and Hofmann, W., "Analysis of radial forces based on rotor eccentricity of bearingless switched reluctance motors," *2010 XIX International Conference on Electrical Machines (ICEM)*, pp. 1–6, Rome, Italy, 6–8 September 2010.

[9] L. Chen, and W. Hofmann, "Modelling and Control of One Bearingless 8/6 Switched Reluctance Motor with Single Layer of Winding Structure," *Proc.14th European Conference on Power Electronics and Applications*, 2011, pp. 1-9.

[10] Chen, L., and Hofmann, W., "Speed regulation technique of one bearingless 8/6 switched reluctance motor with simpler single winding structure," *IEEE Trans. Ind. Electron*., Vol. 59, No. 6, pp. 2592–2600, June 2012.

[11] Lin, F.C., and Yang, S.M., "Self-bearing control of a switched reluctance motor using sinusoidal currents," *IEEE Trans. Power Electronics*, Vol. 22, No. 6, pp. 2518–2526, November 2007.

[12] Cao, X., Deng, Z., Yang, G., and Wang, X., "Independent Control of Average Torque and Radial Force in Bearingless Switched Reluctance Motors with Hybrid Excitations," *IEEE Transactions on Power Electronics*, Vol.24, No.5, pp.1376-1385, May 2009.

[13] Khoo, W. K. S., "Bridge Configured Winding for Polyphase Self-Bearing Machines," *IEEE Transactions on Magnetics*, vol. 41, no. 4, pp. 1289-1295, 2005.

[14] Khoo, W. K. S., Kalita, K., and Garvey, S.D., "Practical Implementation of the Bridge Configured Winding for Producing Controllable Transverse Forces in Electrical Machines," *IEEE Transactions on Magnetics*, vol. 47, no.6, pp.1712-1718, June 2011.

[15] Ahmed, F., Kumar, G., Choudhury, M.D., and Kalita, K., "Bridge Configured Wounded Switched Reluctance Motor," *Procedia Engineering*, vol. 144, pp.817-824, 2016.

[16] Ahmed, F., Choudhury, M.D., Kumar, G., and Kalita, K., "Modeling and Analysis of Bearingless Switched Reluctance Motor Equipped with Specialized Stator Winding," *2016 IEEE International Conference on Power Electronics, Drives and Energy Systems (PEDES)*, pp.1-6, Trivandrum, India, 14-17 December, 2016.

[17] Choudhury, M.D., Ahmed, F., Kumar, G., Kalita, K., and Tammi, K., "Design methodology for a special single winding based bearingless switched reluctance motor," *Journal of Engineering*, *IET*, DOI.10.1049/joe.2016.0368, ISSN 2051-3305, pp.1-11, 2017.

[18] Ahmed, F., Saikia, D., Chatterjee, S., Singh, H., Kashyap, P., and Kalita, K., "Self-Bearing Switched Reluctance Motor: A Review," *1st International Conference on Power and Energy in NERIST (ICPEN)*, pp.1-6, Nirjuli, 2012.

[19] Wang, X., Ge, B., Wang, J., and Ferreira, F.J.T.E., "Radial Force Analytical Modelling for a Novel Bearingless Switched Reluctance Motor When Considering Rotor Eccentricity," *Electric power Components and Systems*, Vol.42,No.6, pp.544-553, March 2014.

[20] Vijayraghavan, P., "Design of Switched Reluctance Motors and Development of a Universal Controller for Switched Reluctance and Permanent Magnet Brushless DC Motor Drives," PhD Thesis, Virginia Polytechnic Institute and State University, November, 2001.

[21] Krishnan, R., "Switched Reluctance Motor Drives: Modelling, Simulation, Analysis, Design, and Applications," CRC Press, 2001.